Dystrophin conferral using human endothelium expressing HLA-E in the non-immunosuppressive murine model of Duchenne muscular dystrophy

Chang-Hao Cui[1,2], Shunichiro Miyoshi[3], Hiroko Tsuji[3], Hatsune Makino[1], Seiichi Kanzaki[1], Daisuke Kami[1], Masanori Terai[1], Harumi Suzuki[4] and Akihiro Umezawa[1,*]

[1]Department of Reproductive Biology, National Institute for Child Health and Development, Tokyo 157-8535, Japan, [2]Department of Basic Medical Science, Mudanjiang Medical College, Mudanjiang 157011, China, [3]Department of Cardiology, Keio University School of Medicine, Tokyo 160-8582, Japan and [4]Department of Pathology, Research Institute, International Medical Center of Japan, Tokyo 162-8655, Japan

Human leukocyte antigen (HLA)-E is a non-classical major histocompatibility complex class I (Ib) molecule, which plays an important role in immunosuppression. In this study, we investigated the immunomodulating effect of HLA-E in a xenogeneic system, using human placental artery-derived endothelial (hPAE) cells expressing HLA-E in a mouse model. *In vitro* cell lysis analysis by primed lymphocytes in combination with siRNA transfection showed that HLA-E is necessary for inhibition of the immune response. Similarly, *in vivo* cell implantation analysis with siRNA-mediated down-regulation of HLA-E demonstrates that HLA-E is involved in immunosuppression. As hPAE cells efficiently transdifferentiate into myoblasts/myocytes *in vitro*, we transplanted the cells into mdx mice, a model of Duchenne muscular dystrophy. hPAE cells conferred dystrophin to myocytes of the 'immunocompetent' mdx mice with extremely high efficiency. These findings suggest that HLA-E-expressing cells with a myogenic potential represent a promising source for cell-based therapy of patients with muscular dystrophy.

INTRODUCTION

Duchenne muscular dystrophy (DMD) is a severe, recessive X-linked form of muscular dystrophy, characterized by rapid progression of muscle degeneration that eventually leads to loss in ambulation, paralysis and death. The disorder is caused by a mutation in the gene encoding dystrophin, an important structural component of muscle tissues. The absence of intact dystrophin results in destabilization of the extracellular membrane–sarcolemma–cytoskeleton architecture, making muscle fibres susceptible to contraction-associated mechanical stress and degeneration. Skeletal muscles degenerate progressively and irreversibly and are replaced by fibrotic tissues (1). Several protocols have been developed for cell-based therapies, especially using an mdx

mouse model, in which mouse dystrophin is defective due to a single point mutation (2,3).

There is no known cure for DMD. However, use of stem cells or myogenic progenitors holds significant potential as an effective and suitable treatment. Myoblasts represent the natural first choice in cell-based therapy for skeletal muscle due to their intrinsic myogenic commitment. However, myoblasts recovered from muscular biopsies are poorly expandable *in vitro* and rapidly undergo senescence (1). Cells with myogenic potential are present in many other tissues, and these cells readily form skeletal muscle under favourable culture conditions (4). Indeed, cell-based therapy for damaged muscle tissue has already reached the clinical setting, with several types of cell populations being exploited (5,6). Experimental approaches to DMD using animal models have also been

*To whom correspondence should be addressed at: National Institute for Child Health and Development, 2-10-1, Okura, Setagaya, Tokyo 157-8535, Japan. Tel: +81 354947047; Fax: +81 354947048; Email: umezawa@1985.jukuin.keio.ac.jp

extensively investigated, using cells derived from bone marrow (7), synovial membrane (8) and menstrual blood (9).

In any cell-based therapy, donor cells are frequently rejected by recipients when transplanted in an allogeneic combination. Rejection is caused by a mismatch of the human leukocyte antigen (HLA). There are a large number of different alleles of each HLA, so a perfect match of all HLAs between donor cells and host cells is extremely rare. HLA-E, together with HLA-G and HLA-F, is a non-classical major histocompatibility complex class I (MHC Ib) molecule (10), which plays an important role in immunosuppression. Among Ib molecules, HLA-E exhibits a restricted pattern of expression in different cell types (11) and is a ligand of CD94/NKG2 receptors (12,13). The interaction of HLA-E with the inhibitory CD94/NKG2 receptor results in the inhibition of natural killer (NK) cell- and cytotoxic T lymphocyte-dependent lysis (12,14). Uteroplacental immune privilege systems utilize this immunosuppression through production of HLA-E, HLA-F and HLA-G in the uterus and the placenta.

In this study, we investigated the immunomodulating effect of HLA (class Ib) in a xenogeneic combination, using placenta-derived cells expressing HLA-E. Human placental artery-derived endothelial (hPAE) cells conferred dystrophin to myocytes of 'immunocompetent' mdx mice, a model of DMD, doing so with extremely high efficiency.

RESULTS

Derivation of hPAE cells

We successfully cultured a large number of hPAE cells obtained from placental arteries of five donors by the explant culture method (Fig. 1A; see Materials and Methods). hPAE cells with endothelium-like morphology (Fig. 1B) adhered to dishes and were regarded as being population doubling (PD) 0 at day 2. They continued to proliferate until PD 17 at day 20 (Fig. 1C). Cell proliferative capacity was assessed by calculating the total number of PDs (PD level or accumulative PDs) using the formula $\log_{10}$(total number of cells/starting number of cells)/$\log_{10} 2$. Flow cytometric analysis revealed that hPAE cells were positive for CD29 (integrin b1), CD31 (PECAM-1), CD44 (Pgp-1/ly24), CD59, CD73, CD105 and CD166 (ALCAM) and negative for CD45, CD106 (VCAM-1) and CD117 (c-kit) (Fig. 1D and E). Almost all the cells were positive for the endothelial marker CD31 (97.7%), implying that the cells were of endothelial origin. Reverse transcriptase (RT)−polymerase chain reaction (PCR) analysis revealed that hPAE cells expressed the endothelial markers constitutively (Fig. 1F). Immunocytochemical analysis also indicated that the hPAE cells were positive for CD31 and von Willebrand factor (vWF) (Fig. 1G). We next tested whether hPAE cells would form an 'angiogenesis network' when plated on Matrigel. As shown in Figure 1H, culture of hPAE cells on extracellular matrix resulted in vascular tube formation within 6 h. hPAE cells with vascular tube formation were immunocytochemically positive for vascular endothelial growth factor (VEGF) (Supplementary Material, Fig. S1).

Expression of HLA-E in hPAE cells

Since non-classical MHC is involved in immune privilege (10,15), we investigated whether hPAE cells produce HLA-E after exposure to cytokines (16). hPAE cells started to express HLA-E after exposure to cytokines at the transcriptional level (Fig. 2A) and the protein level (Fig. 2B and C). Immunostaining showed that HLA-E was mainly localized in the cytoplasm (Fig. 2B, right). Western blot analysis using anti-HLA-E-specific monoclonal antibody revealed a single discrete band at 42 kDa, consistent with the molecular weight of HLA-E protein (Fig. 2C). Immunoprecipitation analysis of the cell supernatant showed a single band at 37 kDa, consistent with the molecular weight of soluble HLA-E (sHLA-E) protein (Fig. 2D), implying that sHLA-E is secreted.

Myogenic induction of hPAE cells *in vitro*

We then investigated whether hPAE cells are capable of differentiating into skeletal myocytes *in vitro* (Fig. 3). hPAE cells started to exhibit multinucleated myotubes in culture after induction (Fig. 3A). Immunocytochemistry indicated that enhanced green fluorescent protein (EGFP)-labelled multinucleated myotubes were positive for desmin (Fig. 3B) and myosin heavy chain (Fig. 3C and D). Myogenesis of hPAE cells was also analysed by RT−PCR with primers that can amplify human myogenic genes, but not their mouse counterparts. hPAE cells constitutively expressed the myogenin gene and started to express the desmin and MyHC-IIx/d genes after induction (Fig. 3E). We also performed tartrate-resistant acid phosphatase stain for osteoclasts, alkaline phosphatase stain for osteoblasts and Oil red O stain for adipocytes on hPAE cells at 21 days after the start of co-cultivation (Supplementary Material, Fig. S2), but failed to detect positive reaction by these stains.

Direct implantation of hPAE cells into immunocompetent BALB/c mice

To further evaluate the *in vivo* response to hPAE cells, cells were directly injected into the thigh muscles of immunocompetent BALB/c mice (17). For comparison, periosteal cells with low expression of HLA-E were injected in the same manner. Histopathological analysis revealed that the injection of periosteal cells induced an immune response at the injected site (Fig. 4A), but hPAE cells did not (Fig. 4B), suggesting that hPAE cells fail to elicit pro-inflammatory responses in immunocompetent mice. Immunohistochemical analysis, using an antibody specific to human vimentin, revealed that the hPAE cells extensively migrated between muscular fibres (Fig. 4B, lower panels). Immunofluorescent analysis revealed that CD45 and CD3 lymphocytes infiltrated near the (donor) periosteal cells at 2 days after the injection into the Balb/c muscle, and the number of lymphocytes increased at 2 weeks (Fig. 4C). In contrast, CD45- and CD3-positive cells were not detected around the vimentin-positive hPAE cells at 2 weeks. We also performed immunofluorescent analysis and western blot analysis to investigate the expression of HLA-E *in vivo*. hPAE cells expressed HLA-E in the muscle tissues (Fig. 4D and E). Moreover, HLA-E expression
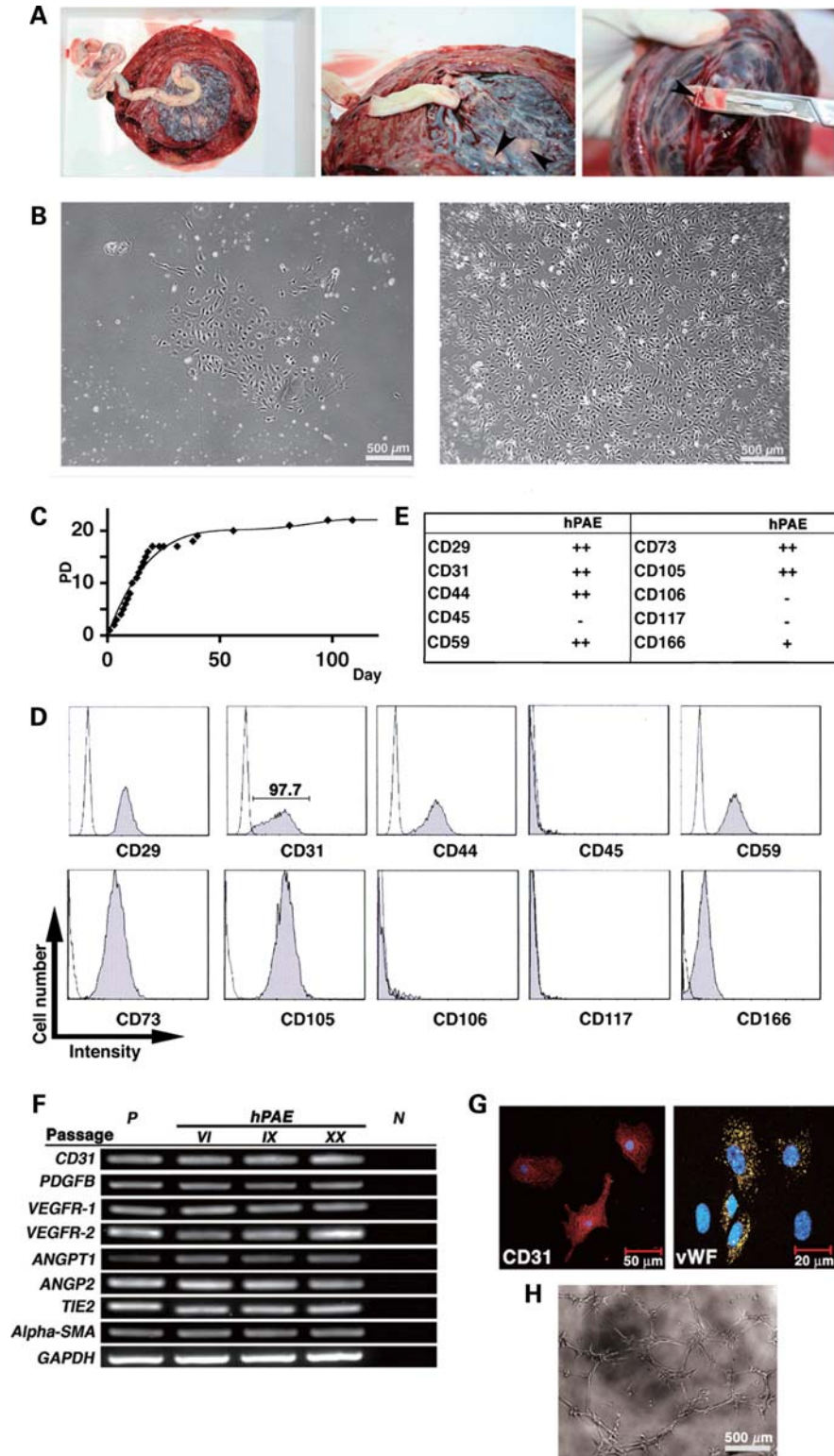
Figure 1. *In vitro* characterization of hPAE cells. (**A**) Macroscopic views showing an explant culture method of hPAE cells. hPAE cells were dissected from isolated placenta arterial vessels (indicated by arrowheads) in human placenta. (**B**) Photos showing morphology of hPAE cells by phase contrast microscopy at primary stages at passage I (left panel: PD 0 and right panel: PD 3). (**C**) Proliferative capacity of hPAE cells. The number of cells was counted with ViCell (Beckman Coulter) at each passage. The total number of PDs (PD level or accumulative PDs) was calculated, using the formula $\log_{10}$(total number of cells/ starting number of cells)/$\log_{10} 2$. (**D**) Flow cytometric profiles indicating expression of several cell surface markers on hPAE cells. (**E**) Scores of peak intensity, compared with isotype controls. '++': strongly positive (10 times and above that of the isotype control), '+': weakly positive (<10 times and twice and above that of the isotype control), '−': negative (less than twice that of the isotype control). (**F**) RT–PCR analysis for endothelial marker expression in hPAE cells at passage VI, IX and XX. The cells were cultured without any inductive stimuli. RNAs from HUVECs and H_2O serve as positive (P) and negative (N) controls, respectively. (**G**) Immunocytochemical analyses of CD31 and vWF in hPAE cells. (**H**) Phase contrast micrograph of *in vitro* endothelial network formation of hPAE cells. hPAE cells were cultured on a basement membrane matrix gel. An 'angiogenesis network' was formed 6 h after cultivation began.
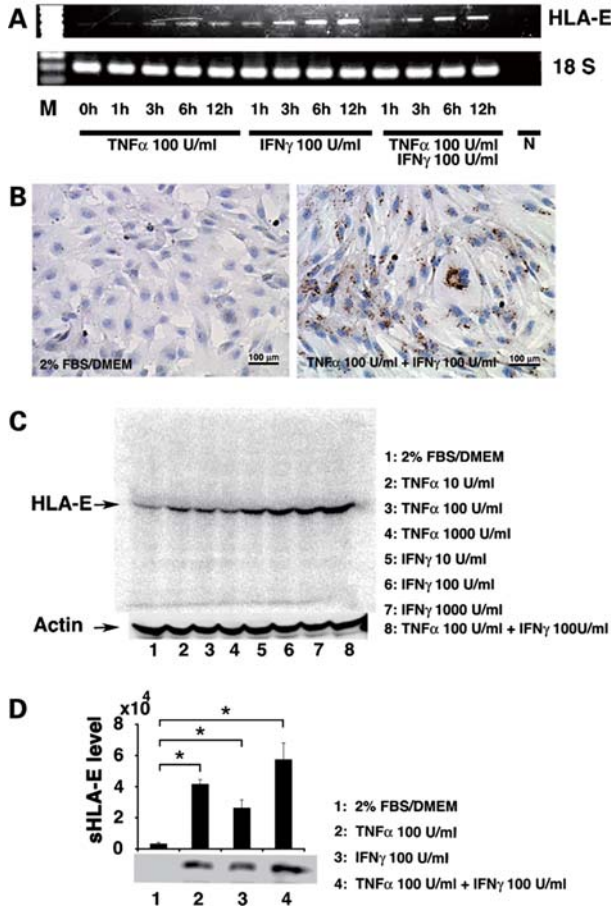
Figure 2. HLA-E mRNA and protein in hPAE cells upon treatment with tumor necrosis factor α (TNFα) and interferon γ (IFNγ). (**A**) RT–PCR showing a time-course of HLA-E expression in response to TNFα and IFNγ. 18S RNA was used as a loading control. M = size markers and N = a negative control in PCR with H_2O. (**B**) Immunocytochemistry of HLA-E localization. The cells were incubated for 24 h with a combination of TNFα and IFNγ at the indicated concentrations (right). Left panel = untreated control. (**C**) Western blot analysis of cell lysates showing levels of HLA-E at 24 h after treatment with TNFα and IFNγ. Combination of two reagents induced more HLA-E at the protein level. Actin was used as a loading control. (**D**) Immuno-precipitation analysis of culture supernatants showing a soluble form of HLA-E (sHLA-E) with exposure to TNFα and IFNγ. sHLA-E level was determined by each signal intensity (mean ± SE). $n = 3$, $^*P < 0.05$.

Figure 3. Myogenic differentiation of hPAE cells under cell culture conditions. (**A**) Photos showing myogenic differentiation of hPAE cells detected by phase contrast microscopy (left) and by fluorescent microscopy (right) in an identical area. EGFP-labelled hPAE cells co-cultured with neonatal murine thymocytes for 21 days. (**B** and **C**) Immunocytochemistry of hPAE cells expressing myogenic markers, desmin (B) and skeletal myosin heavy chain (C, MY32). (**D**) Quantitative analysis of MY32-positive hPAE cells. MY32- and EGFP-double positive cells (no. of MY32+ EGFP+ cells) were counted in 35 mm dishes 3 weeks after induction (mean ± SE). $n = 3$, $^*P < 0.05$. (**E**) RT–PCR showing myocyte-specific genes were expressed along with myogenic differentiation. RT–PCR analysis with PCR primers that amplify only human mRNAs of Myf5, myogenin, desmin and MyHC-IIx/d, but not murine mRNAs. RNAs from human muscle and H_2O served as positive (P) and negative (N) controls, respectively.

remained unchanged over 6 weeks. We then examined interleukin-4 (IL-4), which is essential for transplantation immunity. IL-4 production reached a maximum level after 2 weeks at the injected site and then decreased (Supplementary Material, Fig. S3).

To investigate whether hPAE cells can generate muscle tissue *in vivo*, hPAE cells were implanted directly into the right thigh muscles of BALB/c mice, with phosphate-buffered saline (PBS) being injected at the contralateral muscles as a control. Immunohistochemical analysis was performed using the human-specific antibody at 3 weeks after injection. Myotubes at the injected site expressed human dystrophin as a cluster. No positive reaction was detected in the muscle of BALB/c mice without cell implantation (PBS alone) (Fig. 4E and F; Supplementary Material, Fig. S4). These results imply that dystrophin is transcribed from the dystrophin gene of human donor cells after hPAE
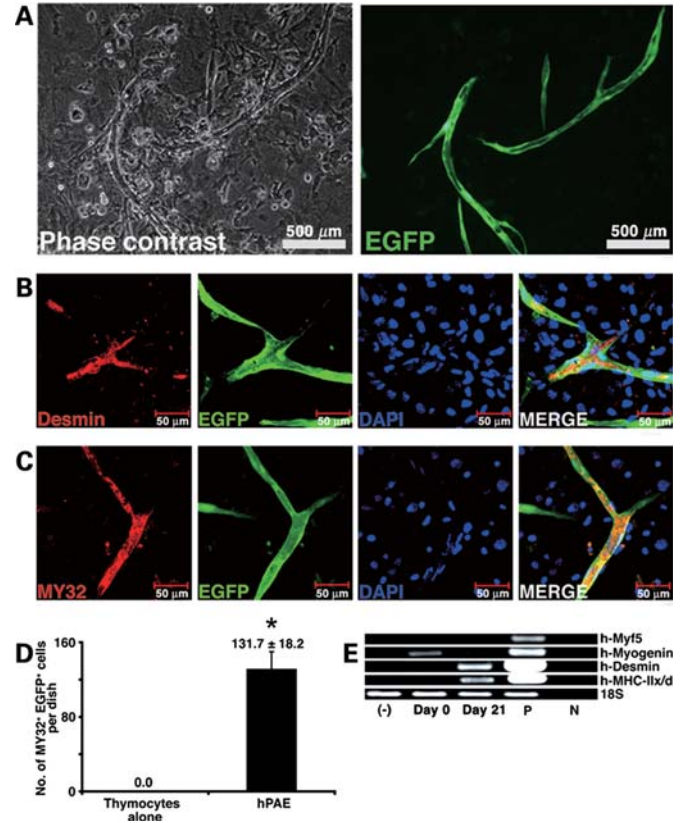
cells differentiated into myotubes and fused to host myocytes without immune response. To determine whether human dystrophin expression in the donor cells is caused by fusion, immunohistochemistry with an antibody against human nuclei (Ab-HuNucl) and 4′,6-diamidino-2-phenylindole (DAPI) stain was performed. We examined almost all the 7 mm thick serial histological sections parallel to the muscular bundle (cross-section) of the muscular tissues by confocal microscopy and found that myocytes had nuclei derived from both human and murine cells in the cross-section (Fig. 4G), implying that dystrophin expression is attributed to fusion between murine host myocytes and human donor cells.

Inhibition of HLA-E by small interfering RNA (siRNA)

To investigate the involvement of HLA-E in immunosuppression, we suppressed HLA-E expression by siRNA in hPAE cells. A significant decrease in HLA-E mRNA was observed
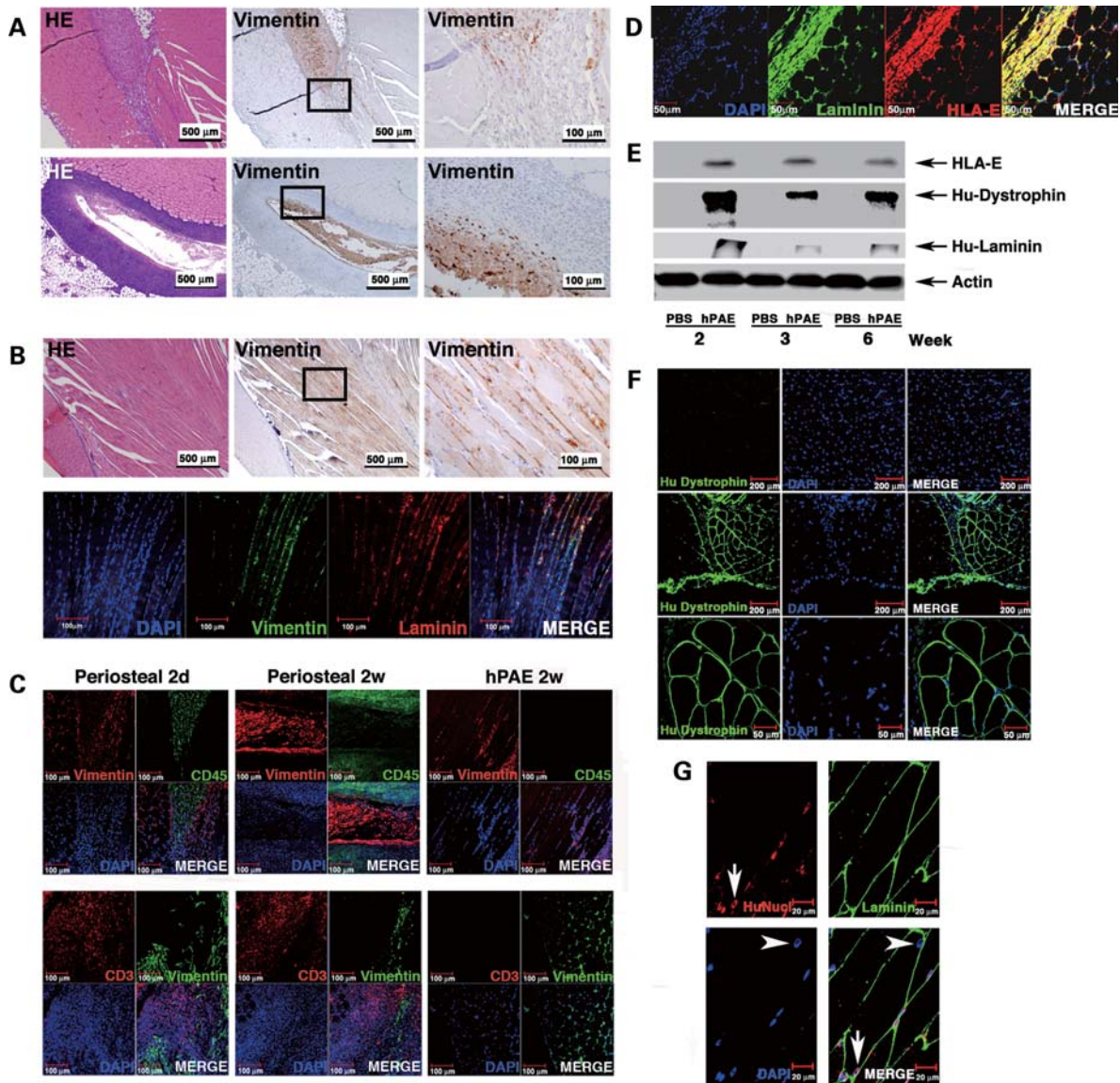
Figure 4. Implantation of hPAE cells into the thigh muscle of BALB/c mice. (**A**) Human periosteal cells (2×10^7 cells) were injected directly into the thigh muscles of BALB/c mice. Immunohistochemical analysis was performed on the muscle section using an antibody against vimentin. Upper panels: 2 days after injection and lower panels: 2 weeks after injection. (**B**) hPAE cells (2×10^7 cells) were injected directly into the thigh muscles of BALB/c mice. Upper panels: immunohistochemistry against vimentin. Lower panels: immunofluorescent analysis. DAPI (blue), vimentin (green), laminin (red) and MERGE (from left to right). (**C**) Immunohistochemical analysis of the thigh muscle sections at 2 days or 2 weeks after injection of human periosteal cells (hPeriosteal) and at 2 weeks after injection of hPAE cells, using antibodies against vimentin (upper panels: red and lower panels: green), leukocyte marker CD45 (green) and T cell marker CD3 (red). (**D**) Immunofluorescent analysis using an antibody against HLA-E (red) and human laminin (green) on the thigh muscle sections at 2 weeks after injection of hPAE cells. (**E**) Western blot analysis of muscle lysates showing levels of HLA-E, dystrophin and laminin. BALB/c mice were implanted with PBS or hPAE cells at the indicated weeks. The level of actin protein was used as a loading control. (**F**) Immunofluorescent analysis using an antibody against human dystrophin (green) on thigh muscle sections 3 weeks after direct injection of hPAE cells (middle and lower panels). PBS was injected into contralateral muscles as a control (upper panels). Dystrophin is totally absent in PBS-injected muscles (upper panels), whereas clusters of muscle fibres display peripheral localization of the dystrophin protein in mice injected with hPAE cells (middle and lower panels). Dystrophin (green), DAPI (blue) and MERGE (from left to right). (**G**) Immunofluorescent analysis using antibodies against laminin (green), human nuclei (HuNucl, red, arrows) and DAPI staining (blue, arrowheads) on thigh muscle sections 3 weeks after injection of hPAE cells.

in the cells transfected with HLA-E siRNA (siHLA-E) when compared with control cells (Fig. 5A). In the same set of experiments, HLA-E protein decreased significantly in siHLA-E-transfected cells when compared with control cells (Fig. 5B). To investigate the involvement of HLA-E in *in vivo* immune response, after pre-treatment with 20 μM siHLA-E for 48 h, hPAE cells were injected into the thigh muscles of immunocompetent BALB/c mice, with hPAE cells treated with control siRNA being injected into the contralateral muscles as a control (Fig. 5C–F). Histopathological analysis revealed that injection of siHLA-E-treated hPAE cells elicited an immune response, as revealed by infiltration of CD3- and CD45-positive lymphocytes in immunocompetent BALB/c mice 7 days after injection, whereas injection of
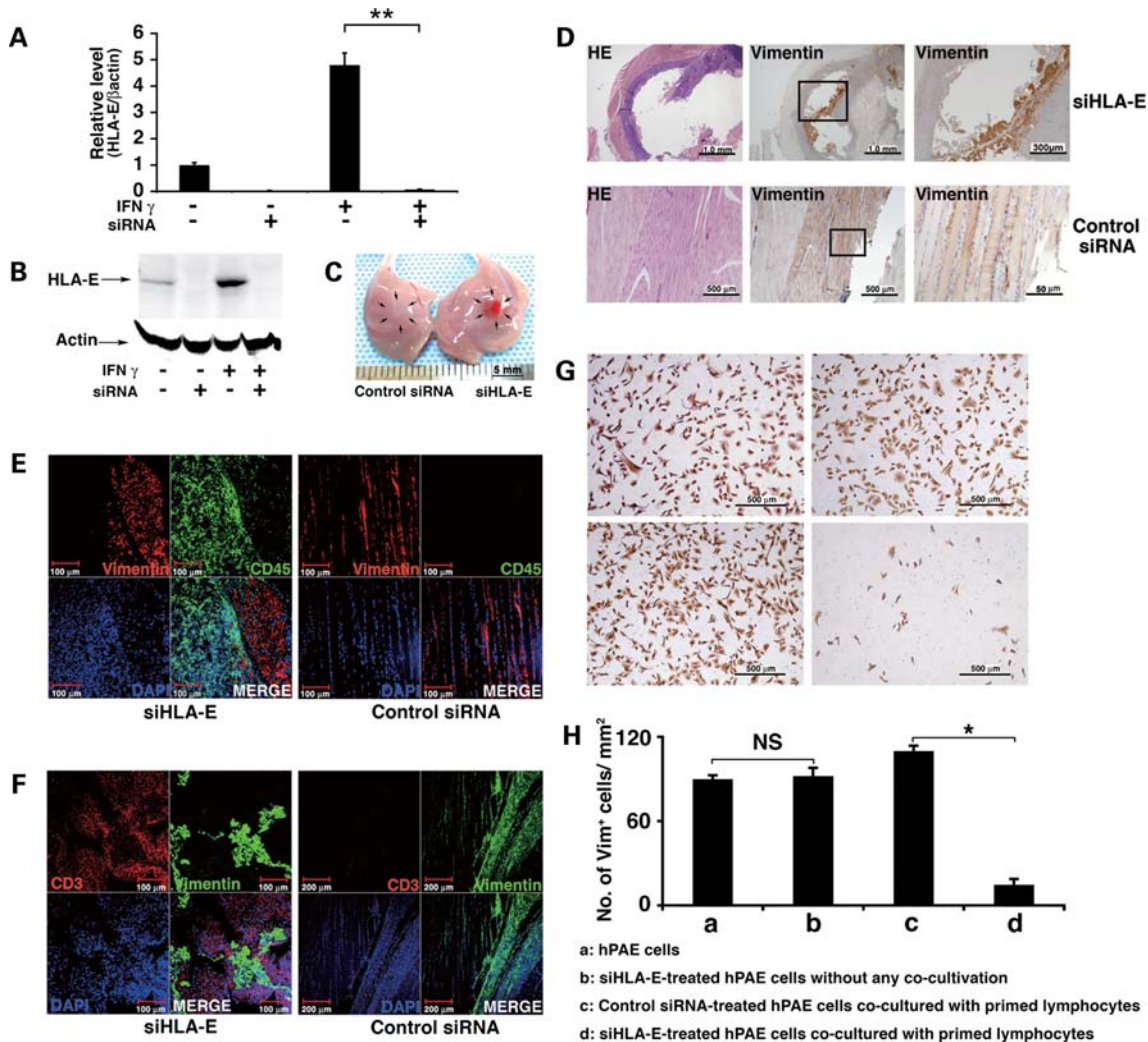
Figure 5. Functional effect of HLA-E siRNA on immunosuppression. (**A**) Inhibition of HLA-E mRNA by siRNA. hPAE cells (1×10^4) grown on 6-well plates were transfected with either control siRNA or HLA-E-specific siRNA (20 μM) for 48 h. HLA-E mRNA levels were quantified using RT–PCR, normalized to β-actin (mean ± SE). $n = 3$, **$P < 0.01$. (**B**) Inhibition of HLA-E protein by siRNA. Whole-cell protein extracts were analysed by SDS–PAGE immunoblotting with antibodies to HLA-E and actin. (**C–F**) siHLA-E-treated hPAE cells and control siRNA-treated hPAE cells were injected into the right and left thigh muscle of BALB/c mice, respectively. Mice were sacrificed 7 days after injection. (C) Injected sites are indicated by arrows (left: control siRNA and right: HLA-E-specific siRNA). (D) Microscopic view (HE stain and immunohistochemistry) of thigh muscles implanted with siHLA-E-treated (upper panels) or control siRNA-treated (lower panels) hPAE cells. (E and F) Immunohistochemical analysis of thigh muscle sections, after injection of siHLA-E-treated or control siRNA-treated hPAE cells and staining with antibodies against vimentin (E: red and F: green), leukocyte marker CD45 (E: green) and T cell marker CD3 (F: red). (**G**) Induction of xenoreactive lysis with spleen-derived lymphocytes. siHLA-E-treated hPAE cells or control siRNA-treated hPAE cells were co-cultured with spleen-derived lymphocytes and immunocytochemically stained for human vimentin. (G) Upper left: hPAE cells, upper right: siHLA-E-treated hPAE cells without any co-cultivation, lower left: control siRNA-treated hPAE cells co-cultured with primed lymphocytes, lower right: siHLA-E-treated hPAE cells co-cultured with primed lymphocytes. (**H**) Survival of hPAE cells after xenoreactive analysis. Vimentin-positive cells (no. of vimentin+ cells/mm^2) significantly decreased in siHLA-E-treated cells when compared with control siRNA-treated cells 3 days after co-incubation with primed lymphocytes. *$P < 0.01$, NS = not significant.

control siRNA-treated hPAE cells did not (Fig. 5E and F). This suggests that HLA-E is necessary for inhibition of an immune reaction *in vivo*. We then investigated whether lysis of hPAE cells by primed lymphocytes is mediated by HLA-E. hPAE cells treated with either siHLA-E or control siRNA were co-cultured with spleen-derived lymphocytes, and induction of xenoreactive lysis was quantified (Fig. 5G and H). siHLA-E-treated hPAE cells were lysed by primed lymphocytes, whereas control siRNA-treated hPAE cells were not, indicating that HLA-E is also necessary for inhibition of the immune response *in vitro*.

Conferral of human dystrophin by cell implantation in the mdx mouse

To investigate whether hPAE cells can confer human dystrophin to myocytes, untreated EGFP-labelled cells were implanted directly into the thigh muscles of mdx mice (Fig. 6A). PBS was injected into the contralateral muscles as a control (Fig. 6B). At 3 weeks after implantation, human dystrophin was detected in EGFP-positive myotubes as a cluster at 18.2% (Fig. 6C). Expression of dystrophin was not caused by reversion to the normal phenotype of dystrophied myocytes
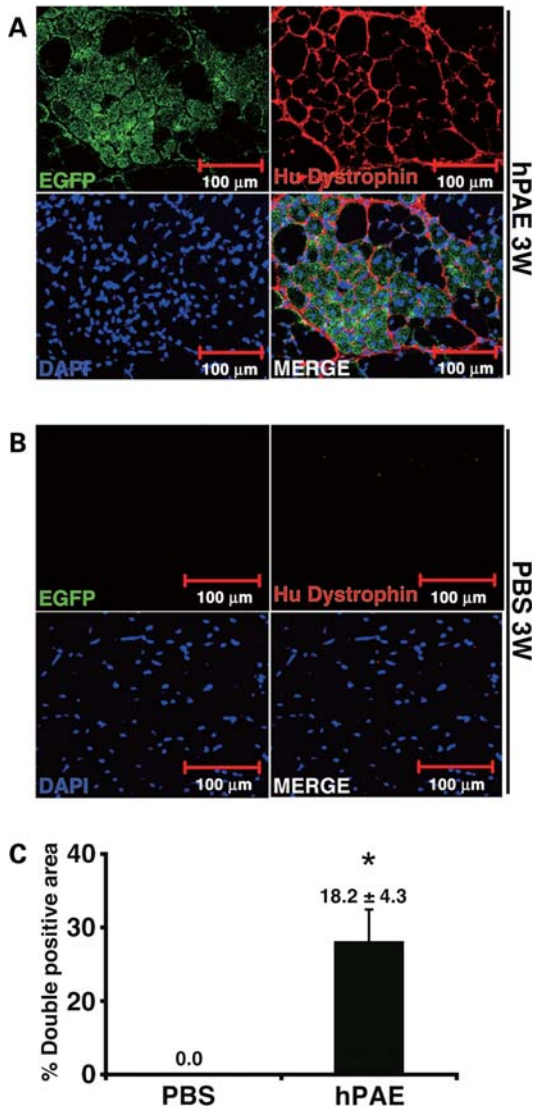
Figure 6. Conferral of dystrophin to mdx myocytes by hPAE cells. (**A**) EGFP-labelled hPAE cells were injected into the thigh muscle of mdx mice. Immunohistochemical analysis revealed the incorporation of implanted cells into newly formed EGFP-positive myofibres (green), which expressed human dystrophin (red) 3 weeks after implantation. (**B**) PBS was injected into contralateral muscles as a control. (**C**) Quantitative analysis of human dystrophin-positive myotubes. The percentage of human EGFP- and dystrophin-positive myofibre areas (% double positive area) was calculated 3 weeks after injection of cells or PBS (mean ± SE). $n = 3$, $^*P = 0.05$.

in the mdx mice because the antibody used in this study is specific to humans. These results suggest that human dystrophin is transcribed from the dystrophin gene of human donor cells.

DISCUSSION

DMD is a devastating X-chromosome-linked muscle disease characterized by progressive muscle weakness attributable to a lack of dystrophin expression at the sarcolemma of muscle fibres (18). There are currently no effective therapeutic approaches for muscular dystrophy. hPAE cells have a high

replicative ability, similar to progenitors or stem cells that display a long-term self-renewal capacity, and had a much higher growth rate in our experimental conditions than marrow-derived stromal cells (19). Immunosuppressive hPAE cells with a direct myogenic potential thus offer significant potential for novel, effective and sustainable cell-based therapy, including when being used in an allogeneic manner. The function of HLA-E has been fully elucidated through its interaction with CD94-NKG2 receptors expressed on NK cells and a subset of T cells (12,13). *In vitro* studies using human cells provided evidence of HLA-E involvement in negative signalling to immune responses (20). Qa-1 (homologous to HLA-E in mice)-deficient mice have defects in immunoregulation mediated by T cells (21). Survival of donor cells in an immunocompetent mouse is attributed, at least partially, to HLA-E-dependent immunosuppression, because knockdown experiments of HLA-E clearly indicate involvement of HLA-E in cell-mediated lysis of hPAE cells (Fig. 5). HLA-E is a protective response of hPAE cells to injury and plays an important role in immunosuppression, irrespective of being either the membrane-bound or soluble form.

It is noteworthy that hPAE cells, as well as other placenta-derived cells, are obtained by a simple, safe and painless procedure, and a large number of hPAE cells can easily be harvested from placental arteries. In this study, we manually separated chorionic large arteries from the chorionic plate that entirely covers the foetal surface of the placenta, which is, in turn, covered by the aminion (Fig. 1A). hPAE cells proliferate over at least PD 17 for >20 days and stop dividing before PD 22. The predicted number of CD31-positive hPAE cells from one placenta of an average size (500 g) would be 1×10^7 (before *ex vivo* amplification), possibly reaching 1×10^{12} after cultivation. This may cover $30\,000\ cm^3$ of muscular tissues in cell-based therapy (5). Cells converted into myotubes *in vitro* at a high frequency after induction, giving rise to large numbers of myofibres expressing human dystrophin when transplanted into BALB/c and mdx mice, thus fulfilling all the criteria required for a successful allogeneic cell therapy for muscular dystrophy.

Compared with previously reported experiments, including from our laboratory (9), the frequency of myotubes with human dystrophin after cell implantation was extremely high. In addition to *in vivo* myogenesis, *in vitro* myogenesis was induced. Myogenin, a helix–loop–helix transcription factor, determines muscle cell fate and accelerates cell fusion, and is constitutively expressed in hPAE cells, implying either that these cells have myogenic potential or that these cells are myogenic progenitors, although their origin is endothelial from the viewpoint of isolation procedure and cell surface markers. Myogenesis may also be promoted by cytokines such as VEGF (22) as well as transcription factors. Furthermore, in cases of cell-based therapy, the so-called 'space' is necessary for survival of implanted donor cells. Irradiation has been used for the generation of space in cases of bone marrow transplantation. Toxin, to induce muscle injury and pathophysiological ischaemia of muscular tissues, can also generate space in muscle (23). BALB/c and mdx mice were used in this study, and almost identical results were obtained from both mice types, although BALB/c mice theoretically do not have any muscular injury. High frequency of human

dystrophin-positive myotube formation may be attributed to the generation of space by the immune response after cell implantation in a xenogeneic combination. hPAE cells produce HLA-E after immunoreaction by production of immunocytokines such as IL-4 (Supplementary Material, Fig. S1), followed by induction of immunosuppression through HLA-E. This immune reaction after cell implantation possibly generates space to enable survival of implanted cells. This possibility is rather favourable because any future cell-based therapy for DMD patients will be employed in an allogeneic combination. In contrast, experimental approaches have been tested in a syngeneic combination, in immunodeficient mice or via use of immunosuppressive drugs. Clinical trials in humans, use an allogeneic combination (5,6), are in no way inferior compared with experimentation with the murine model systems. This study may explain the high frequency of donor cell survival at the implanted sites observed in clinical trials.

Induction of immunosuppression via HLA-E from hPAE cells observed in this study directly leads to the possibility of clinical, allogeneic cell-based therapy. Mesenchymal stem cells (MSCs) or mesenchymal progenitors, isolated from bone marrow as an adherent fibroblast-like population (24), have already been identified in many tissues, including umbilical-cord blood (25), the placenta (26), fat and amniotic fluid (27). They have been used for cell-based therapy because of their self-renewal capacity and their ability to form bone, fat, cartilage, muscle, cardiocytes and neurons (28,29). The isolation of tissue-specific stem cells for expansion *in vitro* and transplantation back into the patient in an allogeneic manner is an ideal strategy, from the viewpoint of industry-based, sustainable supply of large quantities of affordable, quality-controlled cells. Using autologous MSCs to restructure damaged tissues has had some clinical success (30). In most cases of degenerative and genetic diseases, it is unlikely that enough unaffected stem cells will be isolated or available in sufficient quantity, necessitating the use of stem cells from suitable, cost-effective allogeneic sources such as placenta.

MATERIALS AND METHODS

Cultivation of hPAE cells

Human placentas were collected, after delivery, with informed consent. Ethical approval was granted by the Institutional Review Board. To isolate arterial endothelium, we used the explant culture method, in which the cells were outgrown from pieces of placenta arterial vessels (Fig. 1A). Briefly, arterial vessels were separated from arteries in the chorionic plate and chopped into ∼5 mm^3 pieces. The pieces were washed in endothelial basal medium (EBM)-2 (Cambrex, Walkersville, MD, USA) and cultured in endothelial growth medium-2 MV (EGM-2MV; Cambrex), which consisted of EBM-2, 5% foetal bovine serum (FBS) and supplemental growth factors including VEGF, basic fibroblast growth factor, epidermal growth factor and insulin-like growth factor. Arterial vessels attached to the substratum of culture dishes (BD Falcon; Becton Dickinson and Company, San Jose, CA, USA), and cells migrate out from the surface of tissues after 20 days of incubation at 37°C in 5% CO_2. The

cells were harvested with PBS, with 0.1% trypsin and 0.25 mM EDTA, and were re-seeded at a density of 3×10^5 cells in a 10 cm diameter dish. Confluent monolayers of cells were further subcultured. The culture medium was replaced every 3–4 days.

In vitro lentivirus-mediated gene (EGFP) transfer into hPAE cells

Infection of cultured hPAE cells with lentivirus (having a CMV promoter-regulated EGFP reporter plasmid) resulted in high levels of EGFP expression in all cells. EGFP expression was analysed by flow cytometry (31).

Flow cytometric analysis

Flow cytometric analysis was performed as described previously (9). Cells were incubated with primary antibodies or isotype-matched control antibodies followed by immunofluorescent secondary antibody staining. Cells were analysed on an EPICS ALTRA analyser (Beckman Coulter, Fullerton, CA, USA). Antibodies against human CD29, CD31, CD44, CD45, CD59, CD73, CD105, CD106, CD117, CD166 and VEGER (FIk-1) were purchased from Beckman Coulter, Immunotech (Marseille, France), Cytotech (Hellebaek, Denmark) and BD Biosciences Pharmingen (San Diego, CA, USA).

Myogenic differentiation of hPAE cells

A cell suspension was prepared from neonatal murine thymi using frosted slide glasses (MUTO-Glass, Japan). The thymocyte suspension was then washed once in PBS with 2% FBS and filtered through a 100 μm nylon mesh. After centrifugation at 1000 rpm for 5 min, the cell pellet was re-suspended in 10% FBS/Dulbecco's modified Eagle's medium. Floating thymocytes were collected and re-plated at $1 \times 10^6/cm^2$. The next day, hPAE cells were harvested with 0.25% trypsin and 1 mM EDTA and overlaid onto the cultured neonatal thymocytes at $1 \times 10^4/cm^2$. The culture medium was replaced every 2 days with fresh EGM-2 MV.

RT–PCR analysis

Total RNAs (2 μg) were reverse-transcribed with oligo (dT), as described previously (9), and RT–PCR was carried out with primer sets specific for human Myf5, myogenin, desmin, myosin heavy chain-IIx/d (MyHC-IIx/d) (primer sequences are shown in Supplementary Material, Table S1). Human muscle RNAs and H_2O served as positive (P) and negative (N) controls, respectively. The 18S PCR primers were used as a positive control for both human and murine cDNAs. The HLA-E primers (F: CCACCATGGTAGATG GAACCC and R: GCTTTACAAGCTGTCAGACTC) used were the same as those described previously (16). The primer sequences of endothelial cell markers are listed in Supplementary Material, Table S1. Human umbilical vein endothelial cell (HUVEC) RNAs and H_2O served as positive (P) and negative (N) controls, respectively. Glyceraldehyde phosphate dehydrogenase was also used as a positive control.

For quantitative analysis of mRNA levels for HLA-E, the total RNAs were isolated from HLA-E-specific siRNA or control siRNA-transfected hPAE cells using an RNeasy mini-kit (Qiagen, Chatsworth, CA, USA) and were reverse-transcribed by TaKaRa recombinant Taq (Takara Bio Inc., Japan). Real-time PCR was carried out with an ABI PRISM 7000 Sequence Detection System. The 25 µl reaction mixture contained 12.5 µl of SYBR Green PCR Master Mix (TOYOBO, Japan), 10 ng of cDNA template and a primer set for HLA-E, F: CGGCTACTACAATCAGAGCGA and R: CACGCATGTGTCTTCCAGG or for β-action, F: CATG-TACGTTGCTATCCAGGC and R: CTCCTTAATGTCACG-CACGAT. The relative quantification of the transcripts was analysed using the comparative threshold cycle method supplied by the manufacturer.

Immunohistochemical and immunocytochemical analyses

For immunohistochemical analysis (19), the skeletal muscle tissue section slides (paraffin-embedded) were incubated with anti-vimentin monoclonal antibody (clone: V9, Dakocytomation, Glostrup, Denmark) for 1 h at room temperature, followed by horseradish peroxidase (HRP)-conjugated secondary antibody. Staining was detected by diaminobenzidine and H_2O_2. Slides were counterstained with haematoxylin. For the immunofluorescence, antibodies against human dystrophin (NCL-DYS3, Novocastra, Newcastle upon Tyne, UK), GFP (Catalogue no. 632377, Clontech, Mountain View, CA, USA), human nuclei (Catalogue no. MAB1281, Chemicon, Temecula, CA, USA), HLA-E (clone 4D12, MBL, Japan), vimentin, CD45 (leukocyte common antigen) (clone 30-F11, Invitrogen, Camarillo, CA, USA), CD3 (Catalogue no. sc-1127, Santa Cruz Biotechnology, Santa Cruz, CA, USA) and laminin (Mob 202, clone 4C7, DBS, CA, USA; 4H8-2, ab11576, Abcam plc, Cambridge, UK) were used as first antibodies, followed by Alexa-Fluor-conjugated secondary antibodies (Molecular Probes, Eugene, OR, USA).

Immunocytochemical analysis was performed as described previously (19). The antibodies against CD31 (Catalogue no. SCR023, Part no. 2003788, Chemicon), vWF (Catalogue no. SCR023, Part no. 2003787, Chemicon), VEGF (clone EP1176Y, Abcam plc), desmin (clone D9, Catalogue no. 010031, BioScience Products, Emmenbruecke, Switzerland), skeletal myosin (clone MY-32, Sigma-Aldrich, Inc., St Louis, MO, USA), GFP and vimentin were used as first antibodies and Alexa-Fluor-conjugated goat anti-mouse (rabbit) IgG and HRP-conjugated rabbit anti-mouse IgG were used as second antibodies.

Western blotting and immunoprecipitation

Western blot analysis was performed as described previously (19). Blots were incubated with primary antibodies for HLA-E (clone MEM-E/02, Serotec, Oxford, UK), laminin (Mob 202, clone 4C7, DBS) or dystrophin (NCL-DYS3, Novocastra) for 1–2 h at room temperature. After washing, blots were incubated with an HRP-conjugated secondary antibody (0.04 µg/ml) for 30 min. The blots were developed with enhanced chemiluminescence substrate, according to the manufacturer's protocol.

For immunoprecipitation, the supernatants of hPAE cell were incubated with HLA-E antibody (1–2 µg for each sample) for 1 h, followed by incubation with 20 µl of protein A/G plus agarose overnight at 4°C. The supernatants were removed by centrifugation, and the pellets were boiled in 2× sample buffer for 4 min. The products were then applied to sodium dodecyl sulphate (SDS)–polyacrylamide gel electrophoresis (PAGE).

siRNA study

The HLA-E siRNA pool (HLA-E-HSS104836, HLA-E-HSS104837 and HLA-E-HSS104838) was purchased from Invitrogen (Carlsbad, CA, USA) and transfected into hPAE cells using Lipofectamine[TM] RNAiMAX (Invitrogen). Cells were harvested 48 h after transfection and analysed by real-time PCR and western blot.

Xenoreactive immune response

Lymphocytes from BALB/c mouse spleen were isolated by Ficoll/Histopaque density gradient centrifugation. hPAE cells were transfected with either control siRNA or HLA-E-specific siRNA (20 µM) for 48 h. The two cell populations were then co-cultured for 3 days in 2 ml of RPMI supplemented with 10% FBS and 10 U/ml IL-2 (Catalogue no. 212-12, Peprotech Inc., Rocky Hill, NJ, USA). Induction of xenoreactive lysis in the spleen-derived lymphocytes was quantified by immuno-staining with a human-vimentin-specific antibody.

In vivo cell implantation

hPAE cells were implanted into the thigh muscle of 4- to 6-week-old BALB/c (Sankyo Labo Service Corporation, Hamamatsu, Japan) or mdx (C57BL/10ScSn-Dmdmdx/J, Jax Labs, Bar Harbor, ME, USA) mice. For comparison, human periosteal cells were used. The cells (2×10^7) were suspended in PBS in a total volume of 100 µl and injected directly into the thigh muscles. The mice were examined 2 days or 1, 2, 3, 4 and 6 weeks after injection by immunohistochemistry with antibodies against HLA-E, vimentin, laminin and dystrophin. The antibodies for vimentin and dystrophin (NCL-DYS3) are human tissue specific; therefore, they do not react with murine tissues or murine tissue-derived proteins. In addition, siHLA-E (20 µM)-treated or control siRNA-treated hPAE cells were injected directly into the thigh muscle of BALB/c mice.

Statistical analysis

Statistical analysis was performed using the Student's *t*-test. A 95% confidence limit was taken as significant.

SUPPLEMENTARY MATERIAL

Supplementary Material is available at *HMG* online.

REFERENCES

1. Cossu, G. and Mavilio, F. (2000) Myogenic stem cells for the therapy of primary myopathies: wishful thinking or therapeutic perspective? *J. Clin. Invest.*, **105**, 1669–1674.
2. Hoffman, E.P., Brown, R.H. Jr and Kunkel, L.M. (1987) Dystrophin: the protein product of the Duchenne muscular dystrophy locus. *Cell*, **51**, 919–928.
3. Sicinski, P., Geng, Y., Ryder-Cook, A.S., Barnard, E.A., Darlison, M.G. and Barnard, P.J. (1989) The molecular basis of muscular dystrophy in the mdx mouse: a point mutation. *Science*, **244**, 1578–1580.
4. Gerhart, J., Bast, B., Neely, C., Iem, S., Amegbe, P., Niewenhuis, R., Miklasz, S., Cheng, P.F. and George-Weinstein, M. (2001) MyoD-positive myoblasts are present in mature fetal organs lacking skeletal muscle. *J. Cell Biol.*, **155**, 381–392.
5. Skuk, D., Goulet, M., Roy, B., Chapdelaine, P., Bouchard, J.P., Roy, R., Dugre, F.J., Sylvain, M., Lachance, J.G., Deschenes, L. *et al.* (2006) Dystrophin expression in muscles of Duchenne muscular dystrophy patients after high-density injections of normal myogenic cells. *J. Neuropathol. Exp. Neurol.*, **65**, 371–386.
6. Skuk, D., Goulet, M., Roy, B., Piette, V., Cote, C.H., Chapdelaine, P., Hogrel, J.Y., Paradis, M., Bouchard, J.P., Sylvain, M. *et al.* (2007) First test of a 'high-density injection' protocol for myogenic cell transplantation throughout large volumes of muscles in a Duchenne muscular dystrophy patient: eighteen months follow-up. *Neuromuscul. Disord.*, **17**, 38–46.
7. Dezawa, M., Ishikawa, H., Itokazu, Y., Yoshihara, T., Hoshino, M., Takeda, S., Ide, C. and Nabeshima, Y. (2005) Bone marrow stromal cells generate muscle cells and repair muscle degeneration. *Science*, **309**, 314–317.
8. De Bari, C., Dell'Accio, F., Vandenabeele, F., Vermeesch, J.R., Raymackers, J.M. and Luyten, F.P. (2003) Skeletal muscle repair by adult human mesenchymal stem cells from synovial membrane. *J. Cell Biol.*, **160**, 909–918.
9. Cui, C.H., Uyama, T., Miyado, K., Terai, M., Kyo, S., Kiyono, T. and Umezawa, A. (2007) Menstrual blood-derived cells confer human dystrophin expression in the murine model of Duchenne muscular dystrophy via cell fusion and myogenic transdifferentiation. *Mol. Biol. Cell*, **18**, 1586–1594.
10. Carosella, E.D., Paul, P., Moreau, P. and Rouas-Freiss, N. (2000) HLA-G and HLA-E: fundamental and pathophysiological aspects. *Immunol. Today*, **21**, 532–534.
11. Ulbrecht, M., Honka, T., Person, S., Johnson, J.P. and Weiss, E.H. (1992) The HLA-E gene encodes two differentially regulated transcripts and a cell surface protein. *J. Immunol.*, **149**, 2945–2953.
12. Braud, V.M., Allan, D.S., O'Callaghan, C.A., Soderstrom, K., D'Andrea, A., Ogg, G.S., Lazetic, S., Young, N.T., Bell, J.I., Phillips, J.H. *et al.* (1998) HLA-E binds to natural killer cell receptors CD94/NKG2A, B and C. *Nature*, **391**, 795–799.
13. Lee, N., Llano, M., Carretero, M., Ishitani, A., Navarro, F., Lopez-Botet, M. and Geraghty, D.E. (1998) HLA-E is a major ligand for the natural killer inhibitory receptor CD94/NKG2A. *Proc. Natl Acad. Sci. USA*, **95**, 5199–5204.
14. Borrego, F., Ulbrecht, M., Weiss, E.H., Coligan, J.E. and Brooks, A.G. (1998) Recognition of human histocompatibility leukocyte antigen (HLA)-E complexed with HLA class I signal sequence-derived peptides by CD94/NKG2 confers protection from natural killer cell-mediated lysis. *J. Exp. Med.*, **187**, 813–818.
15. Tsuji, H., Miyoshi, S., Ikegami, Y., Hida, N., Asada, H., Togashi, I., Suzuki, J., Satake, M., Nakamizo, H., Tanaka, M. *et al.* (2010) Xenografted human amniotic membrane-derived mesenchymal stem cells are immunologically tolerated and transdifferentiated into cardiomyocytes. *Circ. Res.*, **106**, 1613–1623.
16. Coupel, S., Moreau, A., Hamidou, M., Horejsi, V., Soulillou, J.P. and Charreau, B. (2007) Expression and release of soluble HLA-E is an immunoregulatory feature of endothelial cell activation. *Blood*, **109**, 2806–2814.
17. Faustman, D. and Coe, C. (1991) Prevention of xenograft rejection by masking donor HLA class I antigens. *Science*, **252**, 1700–1702.
18. Mendell, J.R., Kissel, J.T., Amato, A.A., King, W., Signore, L., Prior, T.W., Sahenk, Z., Benson, S., McAndrew, P.E., Rice, R. *et al.* (1995) Myoblast transfer in the treatment of Duchenne's muscular dystrophy. *N. Engl. J. Med.*, **333**, 832–838.
19. Mori, T., Kiyono, T., Imabayashi, H., Takeda, Y., Tsuchiya, K., Miyoshi, S., Makino, H., Matsumoto, K., Saito, H., Ogawa, S. *et al.* (2005) Combination of hTERT and bmi-1, E6, or E7 induces prolongation of the life span of bone marrow stromal cells from an elderly donor without affecting their neurogenic potential. *Mol. Cell. Biol.*, **25**, 5183–5195.
20. Li, J., Goldstein, I., Glickman-Nir, E., Jiang, H. and Chess, L. (2001) Induction of TCR Vbeta-specific CD8+ CTLs by TCR Vbeta-derived peptides bound to HLA-E. *J. Immunol.*, **167**, 3800–3808.
21. Hu, D., Ikizawa, K., Lu, L., Sanchirico, M.E., Shinohara, M.L. and Cantor, H. (2004) Analysis of regulatory CD8 T cells in Qa-1-deficient mice. *Nat. Immunol.*, **5**, 516–523.
22. Bryan, B.A., Walshe, T.E., Mitchell, D.C., Havumaki, J.S., Saint-Geniez, M., Maharaj, A.S., Maldonado, A.E. and D'Amore, P.A. (2008) Coordinated vascular endothelial growth factor expression and signaling during skeletal myogenic differentiation. *Mol. Biol. Cell*, **19**, 994–1006.
23. Darabi, R., Gehlbach, K., Bachoo, R.M., Kamath, S., Osawa, M., Kamm, K.E., Kyba, M. and Perlingeiro, R.C. (2008) Functional skeletal muscle regeneration from differentiating embryonic stem cells. *Nat. Med.*, **14**, 134–143.
24. Friedenstein, A.J., Gorskaja, J.F. and Kulagina, N.N. (1976) Fibroblast precursors in normal and irradiated mouse hematopoietic organs. *Exp. Hematol.*, **4**, 267–274.
25. Bieback, K., Kern, S., Kluter, H. and Eichler, H. (2004) Critical parameters for the isolation of mesenchymal stem cells from umbilical cord blood. *Stem Cells*, **22**, 625–634.
26. In 't Anker, P.S., Scherjon, S.A., Kleijburg-van der Keur, C., de Groot-Swings, G.M., Claas, F.H., Fibbe, W.E. and Kanhai, H.H. (2004) Isolation of mesenchymal stem cells of fetal or maternal origin from human placenta. *Stem Cells*, **22**, 1338–1345.
27. In 't Anker, P.S., Scherjon, S.A., Kleijburg-van der Keur, C., Noort, W.A., Claas, F.H., Willemze, R., Fibbe, W.E. and Kanhai, H.H. (2003) Amniotic fluid as a novel source of mesenchymal stem cells for therapeutic transplantation. *Blood*, **102**, 1548–1549.
28. Prockop, D.J. (1997) Marrow stromal cells as stem cells for nonhematopoietic tissues. *Science*, **276**, 71–74.
29. Kohyama, J., Abe, H., Shimazaki, T., Koizumi, A., Nakashima, K., Gojo, S., Taga, T., Okano, H., Hata, J. and Umezawa, A. (2001) Brain from bone: efficient 'meta-differentiation' of marrow stroma-derived mature osteoblasts to neurons with Noggin or a demethylating agent. *Differentiation*, **68**, 235–244.
30. Horwitz, E.M., Gordon, P.L., Koo, W.K., Marx, J.C., Neel, M.D., McNall, R.Y., Muul, L. and Hofmann, T. (2002) Isolated allogeneic bone marrow-derived mesenchymal cells engraft and stimulate growth in children with osteogenesis imperfecta: implications for cell therapy of bone. *Proc. Natl Acad. Sci. USA*, **99**, 8932–8937.
31. Miyoshi, H., Takahashi, M., Gage, F.H. and Verma, I.M. (1997) Stable and efficient gene transfer into the retina using an HIV-based lentiviral vector. *Proc. Natl Acad. Sci. USA*, **94**, 10319–10323.